Title
Recombinant Major Vault Protein Is Targeted to Neuritic Tips of PC12 Cells

Authors
Herrmann, Christine
Golkaramnay, Elaheh
Inman, Elisabeth
et al.

Peer reviewed

Recombinant Major Vault Protein Is Targeted to Neuritic Tips of PC12 Cells

Christine Herrmann,* Elaheh Golkaramnay,* Elisabeth Inman,‡ Leonard Rome,‡ and Walter Volknandt*

*Biozentrum der J. W. Goethe-Universität, D-60439 Frankfurt/Main, Germany; and ‡Department of Biological Chemistry, University of California, Los Angeles School of Medicine, Los Angeles, California 90024-1737

Abstract. The major vault protein (MVP) is the predominant constituent of ubiquitous, evolutionarily conserved large cytoplasmic ribonucleoprotein particles of unknown function. Vaults are multimeric protein complexes with several copies of an untranslated RNA. Double labeling employing laser-assisted confocal microscopy and indirect immunofluorescence demonstrates partial colocalization of vaults with cytoskeletal elements in Chinese hamster ovary (CHO) and nerve growth factor (NGF)-treated neuronlike PC12 cells. Transfection of CHO and PC12 cells with a cDNA encoding the rat major vault protein containing a vesicular stomatitis virus glycoprotein epitope tag demonstrates that the recombinant protein is sorted into vault particles and targeted like endogenous MVPs. In neuritic extensions of differentiated PC12 cells, there is an almost complete overlap of the distribution of microtubules and vaults. A pronounced colocalization of vaults with filamentous actin can be seen in the tips of neurites. Moreover, in NGF-treated PC12 cells the location of vaults partially coincides with vesicular markers. Within the terminal tips of neurites vaults are located near secretory organelles. Our observations suggest that the vault particles are transported along cytoskeletal-based cellular tracks.

Key words: vaults • protein targeting • major vault protein • transport • PC12

V AULTS, named for their morphology reminiscent of the vaulted ceilings of cathedrals, are ubiquitous, evolutionarily conserved large cytoplasmic ribonucleoprotein particles of unknown function (for review see Kickhoefer et al., 1996). They represent multimeric protein complexes with one predominant member, the major vault protein (MVP).[1] MVP has been characterized in molecular detail in human, rat, electric ray, and cellular slime mold *Dictyostelium discoideum.* It was found to be highly conserved in the animal kingdom (Vasu et al., 1993; Kickhoefer and Rome, 1994; Scheffer et al., 1995; Vasu and Rome, 1995; Herrmann et al., 1997). Highly purified vault particles derived from mammals indicate the presence of uncharacterized minor vault proteins (~54, 192, and 210 kD) (Kedersha and Rome, 1986).

Vault particles also contain several copies of a structurally conserved vault RNA (vRNA). vRNAs (RNA polymerase III products) have been cloned from humans, rats, mice, and bullfrogs (Kickhoefer et al., 1993, 1996, 1998). Although many molecular features of vault particles have been characterized, the function of this large ribonucleoprotein particle remains enigmatic. The identification of the human MVP (initially named LRP for lung resistance–related protein) shed new light on putative cellular functioning of vaults. Numerous multidrug-resistant cancer cells frequently overexpress LRP (Izquierdo et al., 1996) and increased LRP mRNA expression was found to correlate strongly with a predictive value for a multidrug-resistant phenotype (Laurençot et al., 1997). Moreover, it was shown that the vault number is correlated directly to multidrug resistance (Kickhoefer et al., 1998).

An early postulate for vault function was nucleocytoplasmic transport (Rome et al., 1991; Chugani et al., 1993). Vaults have been proposed to constitute the transporter, or the central plugs of the nuclear pore complexes, controlling bidirectional exchange between nucleus and cytoplasm. Regarding the cellular distribution, ~5% of the vault particles are assigned as nucleus-associated and localized to the nuclear pore complex. By conventional immunocytochemistry, most vault particles appear to be uniformly distributed in a punctate pattern throughout the

---

Address correspondence to Walter Volknandt, Department of Neurochemistry, Biocenter, Zoological Institute of J.W. Goethe University, Marie-Curie-Strasse 9, D-60349 Frankfurt/Main, Germany. Tel.: 49-69-798-29603. Fax: 49-69-798-29606. E-mail: volknandt@zoology.uni-frankfurt.de

---

1. *Abbreviations used in this paper:* GLUT4, glucose transporter 4; LRP, lung resistance–related protein; MVP, major vault protein; pvMVP, plasmid encoding VSVG-tagged MVP; SV2, synaptic vesicle protein 2; vMVP, VSVG-tagged MVP; vRNA, vault RNA; VSVG, vesicular stomatitis virus glycoprotein.

cytoplasm in a variety of cells (Izquierdo et al., 1996). Moreover, in rat fibroblasts clusters of vaults are localized at tips of actin filaments in the cell periphery (Kedersha and Rome, 1990). Upon subcellular fractionation vault particles were originally copurified with vesicular structures (Kedersha and Rome, 1986). In the electromotor system of *Torpedo marmorata*, vaults are transported to the nerve terminal where they are allocated near synaptic vesicles (Herrmann et al., 1996; Volknandt and Herrmann, 1997).

To further elucidate the neural aspect of vaults, we analyzed the distribution of vaults in NGF-differentiated PC12 cells with various cellular markers employing laser-assisted confocal microscopy and indirect immunofluorescence. The localization of vaults in neuronlike PC12 cells was compared with vault distribution in CHO cells, a cell line with abundant vaults but lacking the specialized neuronlike cellular differentiation that can be induced in the PC12 cell line. We describe a partial colocalization of vaults with cytoskeletal elements. Moreover, in differentiated PC12 cells location of vaults partially coincides with vesicular markers. Transfection of CHO and PC12 cells with a cDNA encoding the rat MVP containing the viral peptide vesicular stomatitis virus glycoprotein (VSVG) as a tag, demonstrates that the recombinant protein is sorted into vault particles and targeted to the appropriate cell destinations just like endogenous MVPs.

Materials and Methods

Construction of Expression Vectors

The VSVG-tag (YTDIEMNRLGK) was inserted at the NcoI site located directly at the initiation codon at the 5′ end of the cDNA of rat MVP. The resulting cDNA was cloned into the EcoRI site in the mammalian expression vector pcDNA3 (CLONTECH). The engineered construct was named plasmid encoding VSVG-tagged MVP (pvMVP).

Cell Cultures

PC12 cells (phaeochromocytoma cells of rat adrenal medulla origin) were grown in DME supplemented with horse serum (10%) and FCS (5%) at 37°C in the presence of 5% CO_2. CHO cells (derived from ovary cells of the Chinese hamster, *Cricetulus griseus*) were cultivated with Ham's F12 medium supplemented with FCS (10%) at 37°C in the presence of 5% CO_2.

Transfection of PC12 and CHO Cells by Electroporation

PC12 cells were rinsed carefully with 10 ml electroporation buffer (123 mM NaCl, 5 mM KCl, 0.7 mM Na_2HPO_4, 6 mM glucose, 20 mM Hepes, pH 7.05). The cells were removed from the culture flask with 5 ml (two times) electroporation buffer and centrifuged at 300 *g* for 5 min. The supernatant was discarded and the cell pellet was resuspended in 800 μl electroporation buffer. For transfection, the cell suspension was mixed with 50 μg of plasmid DNA in a 4-mm electroporation cuvette. After incubation for 2–5 min at room temperature, electroporation was performed with the following parameters: 500 μF, 310 V, 129 Ω (BTX, Electro cell manipulator 600; Angewandte Gentechnologie Systeme GmbH). The transfected cells were resuspended thoroughly in 20 ml recovery medium (PC12 cell medium as described above supplemented with 3 mM EGTA) and incubated for 30 min at 37°C, 10% CO_2. After centrifugation at 300 *g* for 5 min, the cells were resuspended in 14 ml of medium and grown in culture plates (diam 94 mm) for 48 h in the absence or presence of β-NGF (5 ng/ml; Sigma Chemical Co.). For immunocytochemistry, cells were transferred to poly-D-lysine–coated Permanox coverslips (5 μg/cm²; Sigma Chemical Co.) 24 h after transfection. 1 d after seeding (5.0×10^4 cells/ml), the cells

were processed for immunocytochemistry. Transfection of CHO cells was performed according to the protocol of PC12 cells. In contrast to PC12 cells, CHO cells were treated with a trypsin-EDTA solution (1×, GIBCO BRL) for 1.5 min and resuspended in 30 ml CHO cell medium. After centrifugation at 300 *g* for 5 min, CHO cells were resuspended in 10 ml electroporation buffer and centrifuged a second time using the protocol for PC12 cells. The parameters for the transfection of CHO cells are as follows: 250 μF, 420 V, 129 Ω. For further stimulation of protein expression, sodium butyrate (6 mM) was added 16 h before assaying the cells.

Immunoaffinity Purification of VSVG-Tagged Major Vault Protein (vMVP)

For immunoprecipitation of vMVP from CHO cells magnetic beads conjugated with anti–mouse IgGs (M-450; Dynal) were used. The anti-VSVG IgG1–coated beads were prepared as follows: 10^8 beads were washed in 500 μl PBS (137 mM NaCl, 2.7 mM KCl, 4.3 mM Na_2HPO_4, 1.4 mM KH_2PO_4, pH 7.4) containing 0.1% BSA. Beads were resuspended in 1 ml PBS/0.1% BSA and incubated with 2 μl of anti-VSVG antibody (clone P5D4; Sigma Chemical Co.) for 30 min at room temperature. To remove excess antibody, beads were subsequently washed six times in 1 ml of PBS/0.1% BSA and stored at 4°C overnight.

CHO cells (4 tissue culture dishes of 143 cm²) transfected with the pvMVP plasmid were grown for 48 h. All subcellular fractionation steps were carried out at 4°C. After removal of media, cells were washed twice (5 ml/dish) in buffer A (150 mM NaCl, 1 mM EGTA, 0.1 mM $MgCl_2$, adjusted to pH 7.4 with 10 mM Hepes/NaOH). Cells were mechanically detached using a cell scraper in buffer A (3 ml/dish) containing a cocktail of the following protease inhibitors: antipain, leupeptin, chymostatin (2 μg/ml each), pepstatin (1 μg/ml), and benzamidine (1 mM). Culture dishes were rinsed again with 1 ml of buffer A containing the protease inhibitors. Cell suspensions were centrifuged for 5 min at 375 *g* yielding a pellet fraction (P1) and a supernatant fraction (S1); the latter was stored on ice. P1 was resuspended in buffer A containing the protease inhibitors and thoroughly homogenized by 12 (up and down) strokes in a 0.5-ml glass-Teflon™ homogenizer.

The homogenate was centrifuged for 5 min at 1,000 *g* to yield a postnuclear supernatant (S2). A large amount of intracellular organelles of CHO cells was contained in the supernatant fraction (S1) resulting from a plasma membrane disruption upon detachment of cells. Therefore, S1 was subjected to high speed centrifugation (60 min at 180,000 *g*) to yield the microsomal fraction, P3. P3 was homogenized in 300 μl of buffer A containing the protease inhibitors and combined with S2. The pooled fractions were layered on top of a linear sucrose gradient (4.8 ml, ranging from 0.2 to 1.6 M sucrose) and centrifuged for 60 min at 150,000 *g* in a swinging bucket rotor. Fractions of 300 μl were collected starting from the top of the gradient. The pooled fractions 7–9 (parent fraction) were used for immunoisolation.

Isolation protocol was applied according to the manufacturer's instructions. In brief, anti-VSVG IgG1–coated beads were incubated for 1 h at 4°C with the vault-containing fractions. Beads were washed three times with 500 μl PBS/0.1% BSA. Elution of the immunocomplex was performed in 30 μl of sample buffer (1% glycerol, 2% SDS, 0.0012% bromophenol blue, 0.1 M dithiothreitol, 80 mM Tris/HCl, pH 6.8) by boiling for 5 min in a water bath. Identically treated nontransfected CHO cells served as a control.

Immunocytochemistry

The cellular localization of MVP was investigated using the affinity-purified polyclonal antibody against rat MVP (dilution 1:25; Kedersha and Rome, 1986). The anti-VSV–glycoprotein mAb (1:100; V-5507; clone P5D4; Sigma Chemical Co.) was used to detect the tagged MVP. To compare the cellular distribution of rat MVP with synaptic vesicle markers and cytoskeletal elements the following antibodies and reagents were used: antibody against synaptophysin (1:50; pAb, G95; gift of Dr. Reinhard Jahn, Göttingen, Germany); antibody against VAMP-II/synaptobrevin-2 (1:100; mAb clone 69.1; Synaptic Systems); antibody against the synaptic vesicle protein, SV2 (1:10; mAb, ascites fluid; clone CKK10H, a gift from Dr. Regis B. Kelly, San Francisco, CA; Herrmann et al., 1996); R820, pAb against glucose transporter 4 (GLUT4; 1:50; donated by Dr. Bonzelius, Frankfurt; Herman et al., 1994); β-tubulin (1:40; clone 2-28-33); and phalloidin coupled with TRITC (1:40; both Sigma Chemical Co.) to detect F-actin.

Before fixation the living cells cultivated on Permanox chamber slides

(Nunc) were washed twice with Ringer's solution (155 mM NaCl, 5 mM KCl, 2 mM $CaCl_2$, 1 mM $MgCl_2$, 2 mM NaH_2PO_4, 10 mM glucose, 10 mM Hepes buffer, pH 7.2) at 37°C for 1 min each. The cells were fixed for 7 min in methanol at -20°C and rinsed three times (5 min each) with PBS (137 mM NaCl, 2.7 mM KCl, 4.3 mM Na_2HPO_4, 1.4 mM KH_2PO_4, pH 7.4).

To prevent nonspecific binding of antibodies cells were incubated for 20 min with 5% BSA (Sigma Chemical Co.) in PBS. Primary antibodies were applied for 20 min in the presence of 1% BSA in PBS. After three rinses in PBS for 5 min each, secondary antibodies coupled with fluorescein (1:100; FITC) or rhodamine (1:50; TRITC; both Sigma Chemical Co.) were applied under the same conditions. Finally, the cells were washed three times with PBS (5 min each). The cells were analyzed by using an Axiophot microscope (Zeiss) or a laser-assisted (TCS4D; Leica GmbH) true confocal scanner.

Electrophoretic Techniques

SDS-PAGE was carried out on minigels (10% acrylamide). Immunoblotting was performed using the enhanced chemiluminescence system (ECL; Amersham) according to the manufacturer's instructions.

Northern Blot Analysis

For analyzing length and yield of MVP transcripts, mRNA from CHO or PC12 cells was isolated using an mRNA kit (Oligotex Direct; Quiagen). To further investigate the influence of the differentiation state on the expression of the MVP transcript, PC12 cells were cultivated for 3 d in the presence of β-NGF (5 ng/ml; Sigma Chemical Co.). In addition, mRNA from CHO cells transfected with pvMVP and stimulated with 6 mM butyrate was isolated. mRNA (800 ng each) was separated on a 1% agarose-formaldehyde gel, transferred onto Hybond filters (Amersham Pharmacia Biotech), and hybridized at 68°C in the presence of 5× SSC (0.75 M NaCl, 75 mM sodium citrate, pH 7.0) overnight. A 2.2-kb DIG-labeled RNA deduced from the 3′ end of a rat MVP cDNA clone, isolated from a rat brain Uni-ZAP XR library (Stratagene), was used as a probe. A 1.5-kb DIG-labeled RNA probe, deduced from a mouse β-actin cDNA clone (Stratagene), was used as a control.

Results

Vault Particles Are Abundant in CHO and PC12 Cells

Vaults have been found in all eukaryotic cells analyzed so far with the exception of yeast. The MVP, the predominant member of vaults contributing to >70% of their mass, is abundant both in CHO and PC12 cells. By Western blot analysis using the polyclonal anti–rat vault antibody, one protein band of 104 kD is specifically detected in the total cell homogenates of both cell lines at a similar level (Fig. 1 A). The antibody raised against rat vaults recognizes the MVP in all species investigated; from *Dictyostelium* to humans with molecular masses ranging from 92 to 110 kD (Kedersha et al., 1990; Kickhoefer et al., 1996) indicating a high conservation of the protein. As judged by immunodetection the level of MVP in PC12 cells seems to remain constant over 14 d of culturing time. Moreover, the amount of MVP and its corresponding transcript in PC12 cells appear to be independent of NGF-induced differentiation as estimated by Western and Northern blot analyses (not shown).

In contrast to the yields of immunodetected protein, the expression level of the MVP transcript, as revealed in Northern blots, seems to be much higher in PC12 than in CHO cells (Fig. 1 B). To verify that equal amounts of intact mRNA from both cell lines were loaded, the hybridization signal of the β-actin transcript is shown for comparison (lower panel). In this context it is noteworthy to state that in PC12 cells the 2.2-kb RNA probe of a
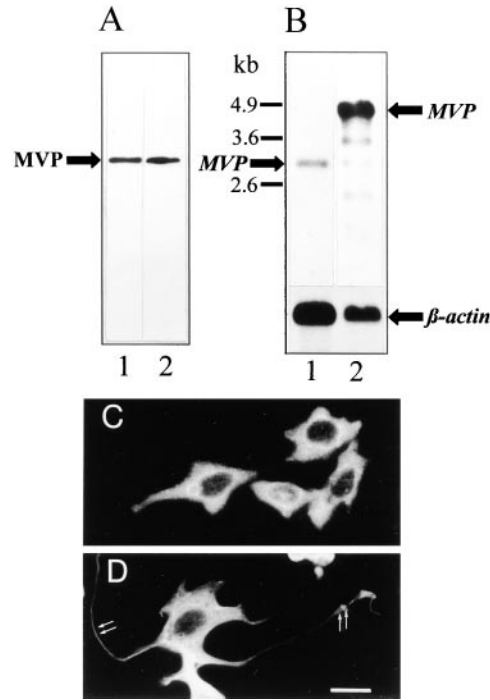

Figure 1. Expression of MVP in CHO and PC12 cells. (A) Western blot of total protein extracts of CHO (lane 1) and PC12 (lane 2) cells using polyclonal affinity-purified anti–rat vault antibody. 50 μg of protein was loaded per lane. (B) Northern blot of mRNA isolated from CHO (lane 1) and PC12 (lane 2) cells using a DIG-labeled RNA encoding rat MVP as a probe. 800 ng of mRNA was applied per lane. The hybridization signal for β-actin (lower graph) served as a control. Sizes of RNA markers are indicated (left). Immunocytochemistry of CHO (C) and PC12 (D) cells using the same antibody as in B demonstrated the overall distribution of vault particles. In D, localization of vaults in neuritic extensions and tips is indicated (arrows). Bar, 20 μm.

rat MVP cDNA clone (comprising 75% of open reading frame from the 3′ end) labels several additional bands albeit less intensely. This hybridization pattern was confirmed in several experiments and did not differ in NGF-treated and untreated PC12 cells (not shown). That the stronger recognition of the MVP-transcript in PC12 cells as compared to CHO cells is not only due to the usage of a rat mRNA probe is revealed in Northern blots using an electric ray mRNA probe yielding a strong hybridization signal with the PC12 MVP transcript (not shown). Thus, signal strength might indeed represent a higher expression level in PC12 than in CHO cells. In the human neuroblastoma cell line, SH-SY5Y, the amount of MVP transcript is lower as compared to PC12 cells and equals that of CHO cells (not shown). Furthermore, MVP transcript size is considerably larger in PC12 than in CHO cells (4.9 versus 3 kb). An MVP transcript size of 4.9 kb was also found in rat brain and human neuroblastoma cells (not shown). In *T. marmorata* the MVP transcript size was ∼2.8 kb (Herrmann et al., 1997). The cDNA clones isolated for sequencing rat, electric ray, or slime mold MVP were ∼2.8 kb in size. A correlation between differences in size and amount of MVP transcripts in various species is not conclusive.

Immunocytochemical analysis demonstrates the abundance of MVP in both cell lines (Fig. 1, C and D). MVP is almost uniformly distributed throughout the entire cytosol. In differentiated PC12 cells labeling of MVP can also be detected in the neuritic extensions including their tips (Fig. 1 D, arrows).

Partial Overlap of Vault and Microtubule Distribution in CHO and PC12 Cells

In double labeling experiments the resolution obtained by conventional indirect immunofluorescence technique proved to be limited. Therefore, we analyzed the cellular distribution of vaults by confocal laser scanning microscopy with 20 serial sections analyzed per cell. Double labeling of CHO cells using antibodies against MVP and β-tubulin demonstrates that vaults are often colocalized with microtubules (Fig. 2, A and B). Vaults reveal a discrete and punctate distribution throughout the cytoplasm (Fig. 2, A and D). The distribution of β-tubulin resembles the typical fiber system of microtubules (Fig. 2, A and B, right). There is a considerable overlap in the distribution of the cytoskeletal fibers and vault particles. High magnification of the cell periphery of CHO cells indicates a predominant orientation of vaults along the cytoskeletal tracks of microtubules (Fig. 2 B). Similarly, in differentiated PC12 cells treated with NGF for 72 h the distribution of MVP overlaps with that of β-tubulin (Fig. 2 C). Especially in the neuritic extensions, the distribution of vaults and microtubules appears to be similar. Staining intensity for β-tubulin in neurites of PC12 cells appears very strong, indicating a dense packaging of microtubules. The evaluation of a putative colocalization of vaults and microtubules remains limited to the soma of PC12 cells where the localization of single particles and fibers can be differentiated. There the majority of vaults are located in the vicinity of microtubules (Fig. 2 C, left).

Overlapping Distribution of Vaults and Filamentous Actin in Neuritic Tips of Differentiated PC12 Cells

The distribution of MVP- and phalloidin-stained filamentous actin in CHO cells is clearly different. Whereas vaults reveal a punctate pattern in thousands of loci throughout the cytoplasm, the actin-based stress fibers are concentrated at the ruffling edges of lamellipodia and span the entire cell as long filaments (Fig. 2 D). In the cell periphery, only a partial overlap of vault and actin filament localization can be observed. Similarly, in differentiated PC12 cells the distribution of vaults and actin filaments differs in the cell soma (Fig. 2 E). However, there is an apparent identical staining pattern of MVP and actin in PC12 cells that is restricted to the most distal areas of neuritic extensions including the tips (Fig. 2 E, inset).

Heterologous Expression of vMVP in CHO and PC12 Cells

To analyze the sorting and targeting of MVP in a narrow time window and to perform further double labeling experiments, we engineered a construct coding for MVP and an additional epitope recognized by an mAb. Transient transfection of CHO and PC12 cells was performed with
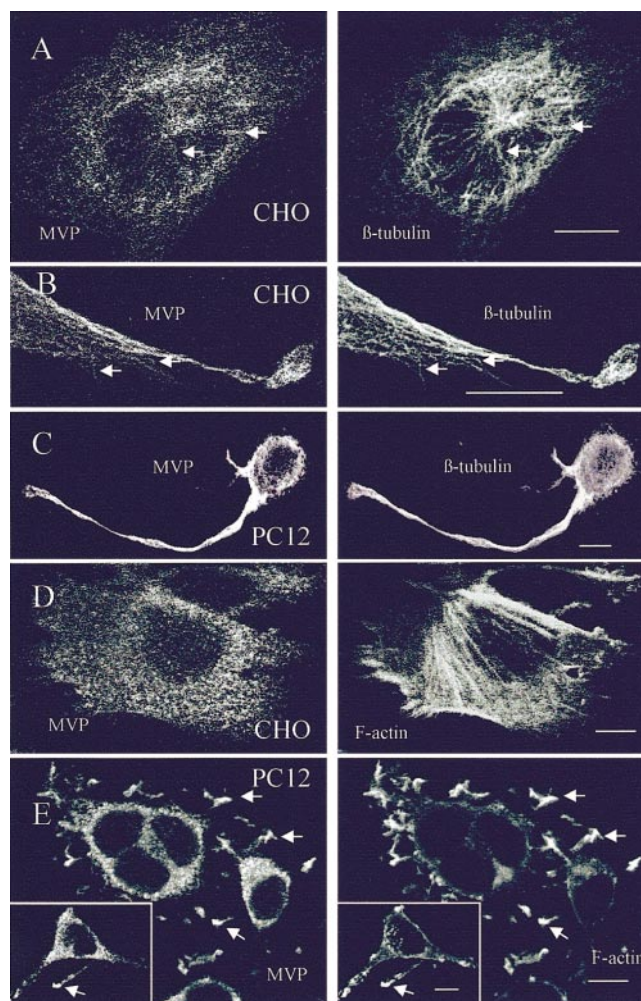

Figure 2. Distribution of vaults and β-tubulin or F-actin in CHO and PC12 cells. The localization was analyzed by double labeling and confocal microscopy of median sections using polyclonal affinity-purified anti–rat vault antibody, anti–β-tubulin mAb, or TRITC-conjugated phalloidin decorating filamentous actin. (A and B) Arrows indicate colocalization of vault particles and microtubules in CHO cells. (C) Overlapping distribution of vaults and microtubules in differentiated PC12 cells is shown. (D) Localization of vaults and filamentous actin in CHO cells. (E) Distribution of vaults and F-actin in PC12 cells is shown. Only in neuritic tips distribution of vaults and F-actin overlap (arrows and inset). Bars, 10 μm.

the plasmid pvMVP (Fig. 3 A) encoding the viral tag VSVG attached to the NH_2 terminus of MVP (vMVP). To differentiate the recombinant protein from the endogenous one, two antibodies were employed. The mAb directed against the VSVG epitope only recognizes the recombinant protein, whereas the pAb against rat MVP detects both the endogenous and the recombinant MVP.

Transfection efficacy of electroporation differed considerably between CHO and PC12 cells. About 30% of CHO cells expressed the recombinant VSVG-tagged protein, whereas only ∼5% of PC12 cells vMVP could be detected by immunocytochemistry. In CHO cells the expression of recombinant and endogenous MVP was evaluated

A

EcoRI NcoI   EcoRI

VSVG-tag   MVP104   pcDNA3

B

kb

3.6 —   ← vMVP

→   ← MVP

2.6 —

1.9 —   ← β-actin

1   2   3

C

kD

112 —   ← MVP*

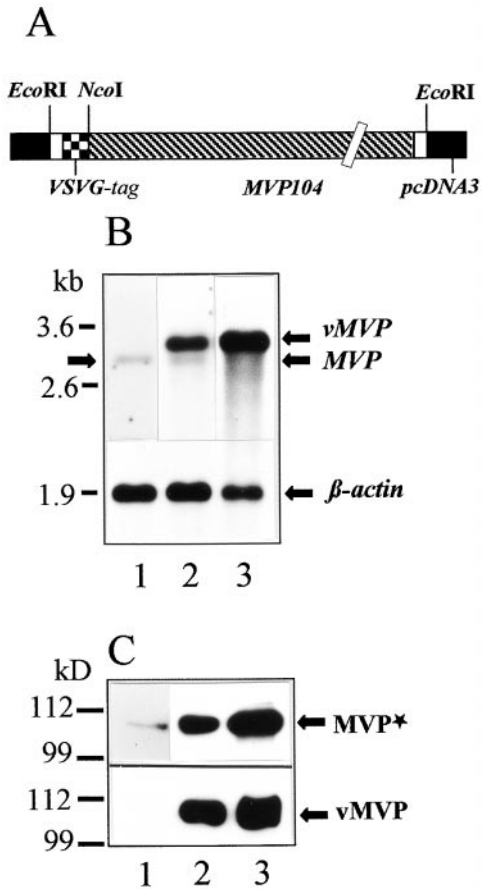99 —

112 —   ← vMVP

99 —

1   2   3

Figure 3. Transient expression of rat vMVP in CHO cells. (A) Schematic drawing of the engineered construct denoted pvMVP for heterologous expression of rat MVP in mammalian cell lines is shown. Note that expression vector and cDNA sequence encoding MVP are not in scale. (B) Northern blot using a DIG-labeled RNA encoding rat MVP as a probe is shown. 800 ng of mRNA was applied per lane. Lane 1 shows mRNA isolated from nontransfected CHO cells; lane 2 shows mRNA from CHO cells transfected with pvMVP; and lane 3 shows mRNA from transfected CHO cells treated with sodium butyrate. The hybridization signal for β-actin (lower graph) served as a control. Arrows indicate the position of the endogenous MVP transcript (left and right), overexpressed vMVP, and β-actin (both right). The position of marker RNA is given in kilobases. (C) Western blot using total protein extract of CHO cells, polyclonal affinity-purified anti–rat vault antibody (upper graph), or anti-VSVG mAb (lower graph) is shown. (Lane 1) Nontransfected; (lane 2) pvMVP-transfected, and (lane 3) pvMVP-transfected and butyrate-treated cells. 30 μg of protein was applied per lane. Protein bands detected by anti-MVP antibody (MVP*) or anti-VSVG antibody (vMVP) are marked by arrows (right). Note, the anti-MVP antibody detects endogenous and recombinant MVP. The size of marker polypeptides is given in kilodaltons (left).

by Western and Northern analyses. The amount of the vMVP transcript is much higher than that of the endogenous MVP transcript (Fig. 3 B). Northern blot analysis reveals a 3.2-kb vMVP transcript. The shift in transcript size occurs because of the attached nucleotides encoding the viral epitope as well as additional nucleotides required for cloning strategies of the pvMVP construct

(Fig. 3 A). Treatment of transfected CHO cells with butyrate results in a further increase of mRNA expression (Fig. 3 B, lane 3). Consistent with the dramatic increase of mRNA expression, de novo synthesis of transiently expressed vMVP far exceeded the amount of endogenous MVP (Fig. 3 C, top, compare lanes 1 and 2). Accordingly, butyrate treatment further stimulates synthesis of vMVP (Fig. 3 C, lane 3).

Immunoisolation of vMVP

To further analyze if recombinant MVP is sorted like endogenous MVP, we investigated the composition of vMVP-containing particles. We immunoisolated vMVP from pvMVP-transfected CHO cells using a anti-VSVG mAb coupled to anti–mouse IgG–coated magnetic beads as a solid support. A combined fraction containing the postnuclear supernatant and microsomes derived from transfected CHO cells (four confluent plates) was subjected to high speed glycerol gradient centrifugation. As analyzed by Western blotting the bulk of vMVP immunoreactivity is retained in fractions 7–9 corresponding to 12–15% glycerol (Fig. 4 A). There is no significant shift of vMVP immunoreactivity compared to total MVP immunoreactivity. Total MVP immunoreactivity of pvMVP-transfected cells seems to shift slightly to denser fractions
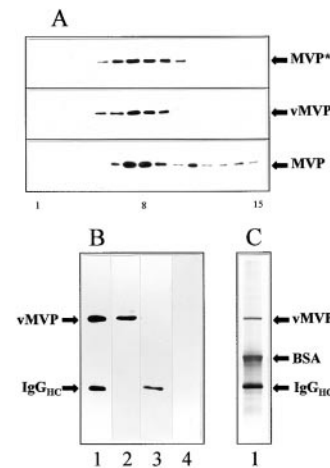

A

← MVP*

← vMVP

← MVP

1   8   15

B   **C**

vMVP →   ← vMVP

     ← BSA

IgG_HC →   ← IgG_HC

1   2   3   4   1

Figure 4. Recombinant MVP is assembled into vault particles: subcellular fractionation (A) and immunoprecipitation of VSVG-tagged major vault protein (B and C). (A) Western blot analysis of the sedimentation behavior of vaults derived from CHO cells on glycerol gradients is shown. The following are shown: (top) Immunodetection of endogenous and recombinant MVP (MVP*) of pvMVP-transfected CHO cells using the anti–rat vault antibody; (middle) immunodetection of vMVP using the anti-VSVG antibody. In the top and middle frames identical fractions were applied per lane. The bottom frame shows immunodetection of endogenous MVP derived from nontransfected cells using the anti–rat vault antibody. Note that both the amount of material loaded per lane as well as the exposure time was doubled in the bottom frame blot as compared to the top two (50:100 μg protein per gradient, 2:4 min exposure time). Fractions of 300 μl were collected from the gradient and analyzed by immunoblotting. The number of fraction is indicated below the graph: starting fraction on top of the gradient (1) vault-enriched fraction (8) and bottom fraction (15). (B) Western blot and (C) silver staining of immunoprecipitate using anti-VSVG mAb and anti–mouse IgG-coated magnetic beads as a solid carrier (lane 1). Bands comprising minor vault proteins are not visible. Parent fraction of transfected cells before immunoisolation (lane 2). Immunoprecipitate of nontransfected CHO cells applying an identical experimental procedure as for transfected cells (lane 3). Parent fraction of nontransfected cells before immunoisolation (lane 4). Positions of vMVP, BSA, and heavy chains of mouse immunoglobulins (IgG_HC) are indicated.

(Fig. 4 A, top, fraction 10). Thus, all vMVP is particulate and no vMVP was found to be soluble (e.g., contained in light fractions in the upper part of the gradient). The sedimentation behavior of vMVP resembles that of endogenous MVP. However, some MVP immunoreactivity smears to denser fractions. This indicates an association of vaults with larger structures (Fig. 4 A, bottom). The lack of immunoreactivity in this region of the gradient in the top frame may occur because of loading less material and a shorter exposure time. The partially purified enriched vault gradient fractions 7–9 were used as starting material for immunoisolation. The isolated immunocomplex contained vMVP as shown by Western blot using the same anti-VSVG antibody employed for immunoisolation (Fig. 4 B, lane 1). Immunoisolation of identically treated nontransfected CHO cells demonstrates specificity of the antibody reaction (Fig. 4 B, lane 3). Silver staining of the eluted immunocomplex reveals vMVP and the presence of additional proteins (Fig. 4 C). The polypeptide pattern of the immunocomplex shows coeluted immunoglobulins (heavy chains ~50 kD), trapped BSA (65 kD; added to prevent nonspecific binding), and several minor bands. This pattern was confirmed in several independent experiments.

Vaults Accumulate in Neuritic Tips of PC12 Cells: Comparison with the Distribution of Neurosecretory Organelles

NGF-treated PC12 cells develop a neuronal phenotype with neurite outgrowth and the appearance of numerous synaptic vesicle-like vesicle. SV2 used as a marker for secretory organelles such as chromaffin granules as well as synaptic vesicle-like vesicles reveal an intense and punctate distribution in the perinuclear region and in the tips of neurites (Fig. 5 A, middle). Consistently, the synaptic vesicle marker, VAMP-II/synaptobrevin-2 present within the same organelles, displays an identical intracellular localization (Fig. 5 B, middle). Double labeling for the vesicle markers and MVP demonstrates a differential distribution of vault particles and secretory organelles in many areas of differentiated PC12 cells. However, in the perinuclear region and in the neurites, especially in the tips, a similar staining pattern of vaults and vesicles could be detected (Fig. 5, A and B, right).

Distribution of vMVP in CHO and PC12 Cells

CHO and PC12 cells analyzed by laser-assisted confocal microscopy and double labeling technique 48 h after trans-
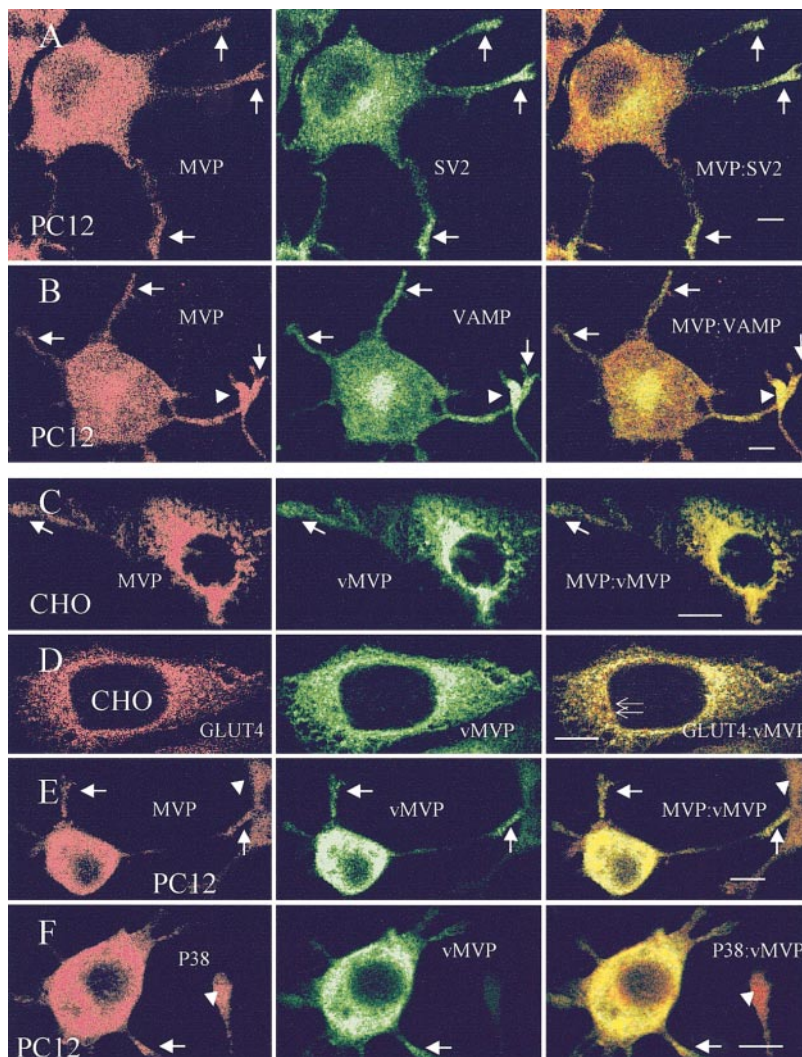

Figure 5. Localization of vault particles and vesicle markers in CHO and PC12 cells. Distribution of endogenous vaults and the synaptic vesicle marker SV2 (A) and VAMP/synaptobrevin (B) in differentiated PC12 cells is shown by double labeling in confocal images of middle sections. Arrows indicate colocalization of secretory organelles and vaults in neuritic tips. Arrowheads indicate immunostained neuritic tip of adjacent cell. An identical distribution of endogenous and recombinant MVP (vMVP) is observed in CHO (C) and differentiated PC12 (E) cells. Note, that antivault antibody (MVP) recognizes both endogenous and recombinant MVP, whereas anti-VSVG mAb only detects vMVP (C and E). Arrows indicate targeting of endogenous and recombinant MVP to cell extensions. Arrowheads indicate processes of neighboring cells revealing no or low expression of vMVP. (D) Localization of vMVP as compared to GLUT4-containing organelles is shown. Thin arrows indicate the differential distribution of GLUT4 and MVP in the perinuclear region of CHO cells. (F) Colocalization of the synaptic vesicle marker P38/synaptophysin and vMVP in neuritic extensions of differentiated PC12 cells (arrows). Arrowheads show the nontransfected cells. Bars, 10 μm.

fection with the pvMVP plasmid demonstrate a high expression of recombinant vMVP (Fig. 5, C–F, middle row). In the transfected cell lines vMVP is distributed like the endogenous MVP (see Fig. 5, A and B). Slight differences in staining intensity of the two antibodies are restricted to the perinuclear region where the recombinant protein appears to be highly concentrated, presumably due to massive de novo synthesis of vMVP and lower affinity of the polyclonal antibody (Fig. 5, C and E, right). Staining of the recombinant protein yields the typical distribution of vaults with the punctate pattern throughout the cytosol. This indicates that vMVP is sorted into vault particles and targeted to the same cellular destinations as endogenous MVP (Fig. 5, C–F, middle, and A and B, left). The recombinant protein is also transported to the cell periphery (Fig. 5, C, E and F, middle, and A and B, left). Arrowheads depict neighboring cells that are either nontransfected and, thus, vMVP negative (Fig. 5 F), or processes of adjacent cells exhibiting only low expression of vMVP (Fig. 5 E).

We compared the distribution of vaults with GLUT4 which is localized in a specific cellular subcompartment. It characterizes a distinct class of intracellular storage vesicles (named surface modifying vesicle) in fat and muscle cells as well as in a variety of transfected cell lines (Herman et al., 1994). A CHO cell line stably transfected with GLUT4 was transiently cotransfected with pvMVP. Fig. 5 D displays the high expression of vMVP as compared to the constitutively expressed GLUT4. Staining for GLUT4 shows the typical intracellular punctate pattern concentrated in the perinuclear area (Fig. 5 D, left). The distribution of vMVP is different from that of GLUT4-containing vesicles. Although the distribution of vMVP is also high in the perinuclear region, the overlap with GLUT4 vesicles is only partial (Fig. 5 D, right). Staining for both markers shows a punctate pattern, although the vMVP-containing loci seem to be larger.

vMVP Is Targeted into Neuritic Tips of Differentiated PC12 Cells

PC12 cells transfected with pvMVP and grown in the presence of NGF for 48 h demonstrate a high expression of vMVP uniformly distributed throughout the cytosol with the characteristic granular appearance (Fig. 5, E and F, middle). Double staining with anti-VSVG antibody recognizing only vMVP and anti-MVP antibody detecting recombinant and endogenous MVP reveals an almost identical distribution of immunolabeling (Fig. 5 E). vMVP is targeted to the tips of neurites as endogenous MVP (Fig. 5 E, arrows, compare to Fig. 5 A, arrows). A neighboring cell with low vMVP expression is depicted by an arrowhead. The synaptic vesicle marker P38/synaptophysin present exclusively on synaptic vesicle-like vesicle is located at the cell soma and transported to neurites in differentiated PC12 cells (Fig. 5 F, left). The distribution of P38/synaptophysin-containing vesicles considerably overlaps with that of vMVP (Fig. 5 F, right). In contrast to SV2 and synaptobrevin that are both localized on chromaffin granules as well as on synaptic vesicle-like vesicle, synaptophysin accumulates in the neurite swellings distant to the tips (Fig. 5 F, left). An extension of an adjacent cell without vMVP expression is depicted by an arrowhead.

Discussion

vMVP Is Sorted into Vault Particles

About 100 copies of MVPs are contained in one single vault particle, whereas only a few copies of the minor constituents contribute to the inventory of vaults (Kedersha et al., 1991). MVPs share a unique domain structure containing an elongated α-helical COOH-terminal tail, numerous phosphorylation motifs, and three repetitive elements (Herrmann et al., 1998).

Electron microscopy reveals that vaults isolated from rat liver, electric ray, rabbit, *Xenopus*, bullfrog, sea urchin, and the lower eukaryote *D. discoideum* are similar both in their dimensions and morphology (Kedersha and Rome, 1990; Hamill and Suprenant, 1997; Volknandt and Herrmann, 1997). Upon subcellular fractionation MVP is entirely retained in a particulate fraction. As shown by negative staining of subcellular fractions, MVP is assembled into intact vaults (Kedersha and Rome, 1986; Kedersha et al., 1990; Volknandt and Herrmann, 1997; Herrmann et al., 1998). Transient transfection of the engineered construct encoding rat vMVP in CHO cells led to a high de novo protein synthesis of the recombinant protein. Although the transfection efficiency was ~30%, the synthesis of the heterologously expressed protein by far exceeded the amount of the endogenous protein.

To further evaluate the components of vault particles containing vMVP we performed immunoisolation of pvMVP-transfected CHO cells using the coexpressed viral tag as target epitope. Western analysis of subcellular fractions demonstrates that vMVP behaving like endogenous MVP is exclusively present in a large complex retained in a particulate fraction. The separation method used gave results in fractionation according to size. Thus, vMVP is likely to be assembled into structures with approximately the same size as vault particles. However, the quantity of the vMVP particles expressed precluded the analysis of their structure using negative staining electron microscopy. The immunocomplex mainly consisted of vMVP, immunoglobulins, and most likely, trapped BSA. In addition, we found several minor bands not characterized yet. Minor constituents of endogenous vault particles have been reported to be proteins of 54, 192, and 210 kD as well as a nontranslatable vRNA of 37 kD (Kedersha and Rome, 1986). Although bands of the isolated immunocomplex migrated at the expected sizes, additional bands of similar or even stronger intensities could not be assigned to the pattern of vault components reported so far (Kickhoefer et al., 1996). Thus, the composition of vMVP-containing vaults is not conclusive.

The assembly of vault particles is probably mediated by the elongated coiled-coil domain at the COOH terminus of MVP (Herrmann et al., 1996). Preliminary experiments with truncated versions of MVP indicate that the COOH terminus is essential for vault assembly. The amount of overexpressed vMVP might far exceed the required cellular content of the minor vault components which gives rise to the formation of vault particles consisting of vMVP and

lacking the other constituents. The contribution of the minor components in highly purified vaults from various species can vary (Kedersha et al., 1990; Herrmann et al., 1996). Consistently, vault formation is limited by the expression of MVP (Kickhoefer et al., 1998). Vaults consisting mainly of vMVP and lacking the others might be a valuable tool to study the relevance of the minor constituents for vault function.

Cellular Distribution of Vaults in CHO and PC12 Cells

Immunocytochemical analysis of transfected CHO and PC12 cells reveals a dense punctate pattern of MVP and vMVP throughout the entire cytoplasm in both cell lines. The granular cytoplasmic appearance of MVP represents the distribution of vault particles. In rat fibroblasts, a punctate cytoplasmic pattern of vault distribution with thousands of vault loci has been reported (Kedersha and Rome, 1990). Both in CHO and PC12 cells, MVP and vMVP are targeted to the cell periphery.

Expression of vMVP is detectable 6 h after transfection of cells. 48 h after transfection vMVP is localized in the neuritic tips of differentiated PC12 cells identical to endogenous MVP. In CHO cells stably transfected with GLUT4 and transiently transfected with vMVP, the localization of GLUT4-containing vesicles and vMVP differs. In contrast, the distribution of MVP/vMVP-containing vaults coincides with markers of secretory organelles in PC12 cells. Double labeling demonstrates a partial colocalization of vaults and secretory organelles in the soma of PC12 cells. Colocalization of vaults and vesicles is obvious in neuritic tips. Markers for secretory vesicles used in this study reside either exclusively on small electron-lucent synaptic vesicle-like vesicles (P38/synaptophysin) or also on large granules (SV2 and VAMP/synaptobrevin) shown recently by immunoelectron microscopical analysis (Marxen et al., 1997). Using the same technique and antibodies against MVP or SV2, a high concentration of vaults and synaptic vesicles was also found in the synaptic terminals of *Torpedo* electromotoneurons near each other (Herrmann et al., 1996).

Vaults Are Associated with Cytoskeletal Elements

Comparison of the distribution of vaults with microtubules in CHO cells reveals a similar pattern in corresponding immunofluorescent images. Vault puncta seem to be oriented along microtubules from the center to the cell periphery. Especially at high magnification, an overlapping distribution of microtubules and vaults in cellular extensions becomes obvious. These observations imply the possibility that vaults, as abundant cytoplasmic particles, are contained in microdomains structurally organized by microtubules and appear to be codistributed. A comparison of the distribution of vaults with filamentous actin in CHO cells reveals a divergent localization. The typical granular cytoplasmic vault distribution differs remarkably from that of polymerized actin organized in long stress fibers and concentrated at focal adhesion points of spreading CHO cells. In spreading fibroblasts, vaults are clustered in localized zones within lamellipodia at actin-rich ruffling edges (Kedersha and Rome, 1990). Furthermore, we compared the distribution of vaults with microtubules or fila-

mentous actin in differentiated PC12 cells that resembled a neuronlike cell type. Overlay of vault and microtubule immunofluorescence in serial sections of PC12 cells yields an almost identical localization of both structures in neurites. In the soma of PC12 cells there is no apparent colocalization of vault particles and actin filaments. However, in the tips of neurites the distribution of vaults and actin fibers seem to overlap completely, yielding an identical pattern of immunostaining. Our immunocytochemical data suggest that there is a cellular transport of vaults mediated by microtubules in the cell soma and neuritic extensions and actin filaments in neuritic tips, where we found colocalization of vaults and secretory organelles.

It has been reported that vaults copurify with microtubules in sea urchin preparations, but the two can be separated by further fractionation. Thus vaults are not considered to be microtubule-associated proteins (Hamill and Suprenant, 1997). The codistribution of vaults with microtubules in cell soma and neurites and the occurrence of vault particles in neuritic tips indicate regulated active cytoplasmic transport. In the neuritic tips, the distribution of vaults resembles that of secretory organelles. In the electric ray, *T. marmorata*, vaults occur in the axon and are abundant in nerve terminals of electromotoneurons implying active axonal transport (Herrmann et al., 1996, 1998; Volknandt and Herrmann, 1997). The dynamic evidence is further supported by crush experiments of the electric nerves demonstrating time-dependent axonal transport with anterograde and retrograde accumulation of vaults (Li et al., 1999).

Cytoplasmic transport of membranous organelles has been studied in a variety of cells. The nerve axon is a good model system for studying organelle transport. Vesicular organelles are axonally transported using microtubules as cellular tracks and motor proteins (for review see Hirokawa, 1998). In addition to the microtubule-dependent mechanism, fast transport of organelles also occurs in the presence of actin filaments (Kuznetsov et al., 1992). Occurrence of polyribosomes and different types of RNA including mRNAs and nonmessenger RNAs in dendrites has been reported (Steward et al., 1996a). There is evidence that mRNA is transported as part of a larger structure on cytoskeletal elements (Taneja et al., 1992; Ferrandon et al., 1994; Carson et al., 1997). Proteins encoded by dendritic mRNA belong to diverse classes representing kinases, cytoskeletal components, and receptors.

The axonal compartment of mammals has been thought to be devoid of mRNA. Recently in the neurosecretory axons of the hypothalamo-neurohypophyseal system, mRNAs encoding vasopressin, oxytocin, prodynorphin, and a neurofilament protein species have been identified (for review see Steward et al., 1996b, 1997). mRNA anchoring to actin filaments (fibroblasts) and also to microtubules (neurons) has been demonstrated (Taneja et al., 1992; Bassel et al., 1994a,b). Reports about transport of nonmessenger RNAs are rare. Neural BC1 RNA, a small polymerase III transcript of unknown function, is preferentially expressed in the brain and is distributed to neuronal dendrites (Tiedge et al., 1991). Moreover, BC1 RNA, a component of a 10S ribonucleoprotein particle, is transported in hypothalamo-neurohypophyseal axons (Kobayashi et al., 1991; Tiedge et al., 1993). Interestingly, it has been reported that BC1

RNA contains elements capable of linking a subset of mRNAs to microtubules presumably by controlling RNA transport along dendritic microtubules (Muramatsu et al., 1998). Little is known concerning the transport mechanisms of RNA particles. Kinesin antisense oligonucleotides inhibit the transport of myelin basic protein mRNA in processes of cultured oligodendrocytes (Carson et al., 1997). RNA was found to be associated with granules. In cultured neurons, RNA granules were transported in anterograde and retrograde direction. The motility had characteristics of an organelle that might be actively transported along cytoskeletal tracks (Knowles et al., 1996). Vaults are by far the largest ribonucleoprotein particles transported to nerve endings and neuritic tips. Our data propose that in neuronlike cell type, vaults may have additional specialized function.

Our findings provide new insights into the cellular distribution of an organelle, which recently has begun to attract attention in different areas of cell biology. The occurrence and abundance of this large cytoplasmic ribonucleoprotein particle in eukaryotic cells argue for an important general function. This is further supported by the high phylogenetic conservation of its main component, the MVP. Cytoplasmic transport of vaults may be required for the various physiological functions postulated so far. A clinical relevance of the human MVP in the prediction of multidrug resistance phenotype in numerous cancer cell lines is well documented. Upregulation of MVP and vaults is a predictor of the multidrug resistance phenotype, but the cellular mechanisms are not understood.

Although there is no preferential localization of vaults to the nuclear envelope, a functional role in nucleocytoplasmic exchange has been proposed. An involvement of vaults in intracellular traffic might be mediated by binding to other cellular organelles or targets. Recently, an interaction of vaults with intracellular steroid hormone receptors has been reported (Abbondanza et al., 1998). The active nucleocytoplasmic shuttle might depend on interaction with members of the nuclear receptor superfamily. To obtain insights in the regulation of intracellular transport of vaults on cytoskeletal tracks is a future challenge. The targeting of this large ribonucleoprotein particle to the cell periphery implies new aspects of the functioning of vaults.

References

Abbondanza, C., V. Rossi, A. Roscigno, L. Gallo, A. Belsito, G. Piluso, N. Medici, V. Nigro, A.M. Molinari, B. Moncharmont, and G.A. Puca. 1998. Interaction of vault particles with estrogen receptor in the MCF-7 breast cancer cell. *J. Cell Biol.* 141:1301–1310.

Bassel, G.J., C.M. Powers, K.L. Taneja, and R.H. Singer. 1994a. Single mRNAs visualized by ultrastructural in situ hybridization are principally localized at actin filament intersections in fibroblasts. *J. Cell Biol.* 126:863–876.

Bassel, G.J., R.H. Singer, and K.S. Kosik. 1994b. Association of poly(A+) mRNA with microtubules in cultured neurons. *Neuron.* 12:571–582.

Carson, J.H., K. Worboys, K. Ainger, and E. Barbarese. 1997. Translocation of myelin basic protein mRNA in oligodendrocytes requires microtubules and kinesin. *Cell Motil. Cytoskel.* 38:318–328.

Chugani, D.C., L.H. Rome, and N.L. Kedersha. 1993. Evidence that vault ribonucleoprotein particles localize to the nuclear pore complex. *J. Cell Sci.* 106: 23–29.

Ferrandon, D., L. Elphick, C. Nüsslein-Volhard, and D. St. Johnston. 1994. Staufen protein associates with the 3′UTR of bicoid mRNA to form particles that move in a microtubule-dependent manner. *Cell.* 79:1221–1232.

Hamill, D.R., and K.A. Suprenant. 1997. Characterization of the sea urchin major vault protein: a possible role for vault ribonucleoprotein particles in nucleocytoplasmic transport. *Dev. Biol.* 190:117–128.

Herman, G.A., F. Bonzelius, A.-M. Cieutat, and R.B. Kelly. 1994. A distinct class of intracellular storage vesicles, identified by expression of the glucose transporter GLUT4. *Proc. Natl. Acad. Sci. USA.* 91:12750–12754.

Herrmann, C., W. Volknandt, B. Wittich, R. Kellner, and H. Zimmermann. 1996. The major vault protein (MVP100) is contained in cholinergic nerve terminals of electric ray electric organ. *J. Biol. Chem.* 271:13908–13915.

Herrmann, C., H. Zimmermann, and W. Volknandt. 1997. Analysis of a cDNA encoding the major vault protein from the electric ray *Discopyge ommata. Gene.* 188:85–90.

Herrmann, C., R. Kellner, and W. Volknandt. 1998. Major vault protein of electric ray is a phosphoprotein. *Neurochem. Res.* 23:39–46.

Hirokawa, N. 1998. Kinesin and dynein superfamily proteins and the mechanism of organelle transport. *Science.* 279:519–526.

Izquierdo, M.A., G.L. Scheffer, M.J. Flens, G. Giacone, H.J. Broxterman, C.J.M. Meijer, P. van der Valk, and R.J. Scheper. 1996. Broad distribution of the multi-drug resistance-related vault lung resistance protein in normal human tissues and tumors. *Am. J. Pathol.* 148:877–887.

Kedersha, N.L., and L.H. Rome. 1986. Isolation and characterization of a novel ribonucleoprotein particle: large structures contain a single species of small RNA. *J. Cell Biol.* 103:699–709.

Kedersha, N.L., and L.H. Rome. 1990. Vaults: large cytoplasmic RNP's that associate with cytoskeletal elements. *Mol. Biol. Rep.* 14:121–122.

Kedersha, N.L., M.C. Miquel, D. Bittner, and L.H. Rome. 1990. Vaults. II. Ribonucleoprotein structures are highly conserved among higher and lower eukaryotes. *J. Cell Biol.* 110:895–901.

Kedersha, N.L., J.E. Heuser, D.C. Chugani, and L.H. Rome. 1991. Vaults. III. Vault ribonucleoprotein particles open into flower-like structure with octagonal symmetry. *J. Cell Biol.* 112:225–235.

Kickhoefer, V.A., and L.H. Rome. 1994. The sequence of a cDNA encoding the major vault protein from *Rattus norvegicus. Gene.* 151:257–260.

Kickhoefer, V.A., R.P. Searles, N.L. Kedersha, M.E. Garber, D.L. Johnson, and L.H. Rome. 1993. Vault ribonucleoprotein particles from rat and bullfrog contain a related small RNA that is transcribed by RNA polymerase III. *J. Biol. Chem.* 268:7868–7873.

Kickhoefer, V.A., S.K. Vasu, and L.H. Rome. 1996. Vaults are the answer, what is the question? *Trends Cell Biol.* 6:174–178.

Kickhoefer, V.A., K.S. Rajavel, G.L. Scheffer, W.S. Dalton, R.J. Scheper, and L.H. Rome. 1998. Vaults are up-regulated in multidrug-resistant cancer cell lines. *J. Biol. Chem.* 273:8971–8974.

Knowles, R.B., J.H. Sabry, M.E. Martone, T.J. Deerinck, M.H. Ellisman, G.J. Bassell, and K.S. Kosik. 1996. Translocation of RNA granules in living neurons. *J. Neurosci.* 16:7812–7820.

Kobayashi, S., S. Goto, and K. Anzai. 1991. Brain-specific small RNA transcript of the identifier sequences is present as a 10S ribonucleoprotein particle. *J. Biol. Chem.* 266:4726–4730.

Kuznetsov, S.A., G.M. Langford, and D.G. Weiss. 1992. Actin-dependent organelle movement in squid axoplasm. *Nature.* 356:722–725.

Laurençot, C.M., G.L. Scheffer, R.J. Scheper, and R.H. Shoemaker. 1997. Increased LRP mRNA expression is associated with the MDR phenotype in intrinsically resistant human cancer cell lines. *Int. J. Cancer.* 72:1021–1026.

Li, J.-Y, W. Volknandt, A. Dahlström, C. Herrmann, J. Blasi, B. Das, and H. Zimmermann. 1999. Axonal transport of ribonucleoprotein particles (Vaults). *Neuroscience.* In press.

Marxen, M., V. Maienschein, W. Volknandt, and H. Zimmermann. 1997. Immunocytochemical localization of synaptic proteins at vesicular organelles in PC12 cells. *Neurochem. Res.* 22:941–950.

Muramatsu, T., A. Ohmae, and K. Anzai. 1998. BC1 RNA protein particles in mouse brain contain two Y-, H-element-binding proteins, translin and a 37 kDa protein. *Biochem. Biophys. Res. Commun.* 247:7–11.

Rome, L., N. Kedersha, and D. Chugani. 1991. Unlocking vaults: organelles in search of a function. *Trends Cell Biol.* 1:47–50.

Scheffer, G.L., P.L. Wijngaard, M.J. Flens, M.A. Izquierdo, M.L. Slovak, H.M. Pinedo, C.J. Meijer, H.C. Clevers, and R.J. Scheper. 1995. The drug resistance-related protein LRP is the human major vault protein. *Nat. Med.* 1:578–582.

Steward, O. 1997. mRNA localization in neurons: a multipurpose mechanism? *Neuron.* 18:9–12.

Steward, O., P.M. Falk, and E.R. Torre. 1996a. Ultrastructural basis for gene expression at the synapse: synapse-associated polyribosome complexes. *J. Neurocytol.* 25:717–734.

Steward, O., R. Kleiman, and G. Banker. 1996b. Subcellular localization of mRNA in neurons. *In* Molecular Biology Intelligence Unit Series: Localized RNAs. H.D. Lipshitz, editor. CRC Press. Boca Raton, FL. 235–255.

Taneja, K.L., L.M. Lifshitz, F.S. Fay, and R.H. Singer. 1992. Poly(A+) RNA codistribution with microfilaments: evaluation by in situ hybridization and quantitative digital imaging microscopy. *J. Cell Biol.* 119:1245–1260.

Tiedge, H., R.T. Fremeau, P.H. Weinstock, O. Arancio, and J. Brosius. 1991. Dendritic localization of neural BC1 RNA. *Proc. Natl. Acad. Sci. USA.* 88: 2093–2097.

Tiedge, H., A. Zhou, N.A. Thorn, and J. Brosius. 1993. Transport of BC1 RNA in hypothalamo-neurohypophyseal axons. *J. Neurosci.* 13:4214–4219.

Vasu, S.K., and L.H. Rome. 1995. *Dictyostelium* vaults: disruption of the major proteins reveals growth and morphological defects and uncovers a new associated protein. *J. Biol. Chem.* 270:16588–16594.

Vasu, S.K., N.L. Kedersha, and L.H. Rome. 1993. cDNA cloning and disruption of the major vault protein α gene (*mvp*A) in *Dictyostelium discoideum.* *J. Biol. Chem.* 268:15356–15360.

Volknandt, W., and C. Herrmann. 1997. The major protein of a large ribonucleoprotein particle (VAULT) is localized in nerve terminals. *In* Neurochemistry: Cellular, Molecular, and Clinical Aspects. A.W. Teelken and J. Korf, editors. Plenum, London. 675–681.